Dalton Transactions

ROYAL SOCIETY OF CHEMISTRY

PAPER

View Article Online
View Journal | View Issue

Check for updates

Cite this: *Dalton Trans.*, 2022, **51**, 1137

Rational design of carborane-based Cu_2-paddle wheel coordination polymers for increased hydrolytic stability†‡

Zhen Li,[a] Duane Choquesillo-Lazarte,[b] Julio Fraile,[a] Clara Viñas,[a] Francesc Teixidor[a] and José G. Planas*[a]

Received 1st December 2021,
Accepted 9th December 2021

DOI: 10.1039/d1dt04065k

rsc.li/dalton

A new unsymmetric carborane-based dicarboxylic linker provided a 1D Cu_2-paddle wheel coordination polymer (**2**) with much higher hydrolytic stability than the corresponding 2D Cu_2-paddle wheel polymer (**1**), obtained from a related more symmetrical carborane-based linker. Both **1** and **2** were used as efficient heterogeneous catalysts for a model aza-Michael reaction but only **2** can be reused several times without significant degradation in catalytic activity.

Introduction

Coordination polymers (CPs), also known as metal–organic frameworks (MOFs) for those that are porous, are materials constructed by connecting inorganic nodes with organic linkers.[1–5] These materials have been rapidly developed over the past decades. The tunable chemical functionality and porosity in the case of MOFs lead to unique properties for a variety of applications.[2,6–15] For the practical applications of these materials, good stability under practical conditions is a prerequisite. Water or moisture is usually present in most industrial processes, such as carbon dioxide capture from flue gas, water purification, proton conduction and many catalytic processes. However, the practical use of MOFs is severely restricted by their molecular sensitivity to water or air humidity due to the labile coordination bonds between metal nodes and ligands.[16–18] The hydrolytic stability of MOFs is governed by multiple intrinsic factors such as coordination environment, metal compositions, oxidation states, nature of organic linkers, interpenetration, flexibility, and framework dimensionality.[16,18–24] Several approaches have been proposed to improve the aqueous stability of MOFs, for example, by strengthening the ligand–metal bonds or by increasing the MOF hydrophobicity.[16,18–26] In recent years we have reported that the introduction of hydrophobic carborane-based linkers into MOFs greatly improves their hydrolytic stability for further practical applications.[27] Icosahedral boranes $[B_{12}H_{12}]^{2-}$ and carboranes 1,*n*-$C_2B_{10}H_{12}$ (*n* = 2, 7 or 12) are a class of commercially available and exceptionally stable 3D-aromatic boron-rich clusters that possess material-favorable properties such as thermal and chemical stability and high hydrophobicity.[28–32] Neutral carboranes are remarkably robust icosahedral boron clusters with two carbon and ten boron atoms. The delocalized electron density is not uniform through the cage, giving rise to extraordinary differences in the electronic effects of the clusters.[33,34] This unusual electronic structure is often highlighted by considering carboranes as inorganic three-dimensional "aromatic" analogs of arenes.[35,36] The spherical nature of these boron clusters, with slightly polarized hydrogen atoms and the presence of hydride-like hydrogens at B–H vertexes, makes carboranes more hydrophobic. Such properties make icosahedral borane and carborane clusters valuable fragments to construct ligands for CPs or MOFs.[37,38] For example, $[B_{12}H_{12}]^{2-}$ provided microporous MOFs with outstanding selectivities in gas separation.[39–42] In pursuit of synthesizing water-resistant MOFs, we are working on the design and preparation of carborane-based ligands.[43–48] The incorporation of such ligands into CPs or MOFs is known to increase their thermal[49–56] and hydrolytic stability.[27,57–60] For example, we have recently reported the most stable Cu-paddle wheel MOF against water in the literature.[27] The extraordinary water stability of this MOF is related not only to the high hydrophobicity of the *m*-carborane ligand **L1** (1,7-di(4-carboxyphenyl)-1,7-dicarba-*closo*-dodecaborane; Chart 1) but also to the interpenetrated 3D structure and the presence of the hydrophobic DABCO (1,4-diazabicyclo[2.2.2]octane) base. The hydrolytic

[a]*Institut de Ciència de Materials de Barcelona, ICMAB-CSIC, Campus de la UAB, 08193 Bellaterra, Spain. E-mail: jginerplanas@icmab.es*
[b]*Laboratorio de Estudios Cristalográficos, IACT, CSIC-Universidad de Granada, Avda. de las Palmeras 4, 18100 – Armilla, Granada, Spain*

†Z. L., D. Ch.-L., J. F. and J. G. Planas dedicate this work to Francesc Teixidor and Clara Viñas for their 70th birthdays and their valuable contributions to the boron cluster chemistry.

‡Electronic supplementary information (ESI) available: Experimental methods, IR, TGA data, and PXRD patterns. CCDC 2119738. For ESI and crystallographic data in CIF or other electronic format see DOI: 10.1039/d1dt04065k

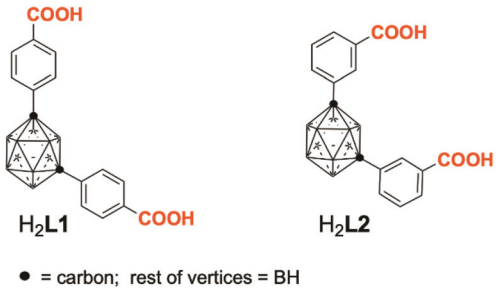

Chart 1

stability is remarkable for a Cu(II) MOF, which in general is among the most unstable transition metal-based MOFs.[61] In the absence of DABCO, **L1** forms a family of 2D coordination polymers $[Cu_2(\mathbf{L1})_2(Solv)_2]\cdot xSolv$ (**1-Solv** = **1-DMF**, **1-DMA** or **1-MeOH**) that are not stable in water.[62] The 2D nature of such coordination polymers expose the Cu-paddle wheel and this makes them more available for hydrolysis or ligand displacements, which again precludes any applications in the presence of water. We reasoned that a more unsymmetrical isomer of **L1**, such as **L2** (1,7-di(3-carboxyphenyl)-1,7-dicarba-*closo*-dodecaborane, Chart 1) could provide a more corrugated structure that increases the hydrolytic stability of the formed Cu(II)-paddle wheel structure while maintaining a significant amount of Cu(II) centers available for applications such as catalysis.

We demonstrate here that the less symmetric ligand **L2** (Scheme 1) has a more corrugated structure than **L1** and it greatly increases the hydrolytic stability of the formed Cu(II)-paddle wheel structure (**2**). As a proof of concept, **1** and **2** were tested as heterogeneous catalysts for a prototype aza-Michael mono-addition reaction. Although both compounds are active catalysts for such a reaction, only compound **2** can be reused at least four times without significant loss in catalytic activity.

Experimental section

Materials and methods

All chemicals were of reagent-grade quality. They were purchased from commercial sources and used as received. All synthetic procedures were carried out in air unless noted otherwise. 1-DMF was synthesized based on our previous report.[62] Thermogravimetric Analysis (TGA) was performed under N_2 on an nSTA 449 F1 Jupiter instrument (heating rate: 10 °C min^{-1}; temperature range: 25 °C to 800 °C). Powder X-ray Diffraction (PXRD) was performed at room temperature on a Siemens D-5000 diffractometer with Cu Kα radiation (λ = 1.5418 Å, 35 kV, 35 mA, increment = 0.02°). An optical microscope (Olympus BX52) was used to monitor the morphology and color changes under various conditions. Gas sorption–desorption (CO_2/273 K and N_2/77 K) measurements were performed using an ASAP2020 surface area analyzer. Samples were first degassed at 120 °C for 24 h. Elemental analyses were performed using a Thermo (Carlo Erba) Flash 2000 Elemental Analyser, configured for wt% CHN. Attenuated total reflection Fourier transform infrared (ATR-FTIR) spectra were recorded using a PerkinElmer Spectrum One spectrometer equipped with a Universal ATR sampling accessory. ^{1}H NMR, ^{11}B NMR, $^{11}B\{^1H\}$ NMR and $^{13}C\{^1H\}$ NMR spectra were recorded on a Bruker Avance-400 spectrometer. Chemical shifts were referenced to the residual solvent peak for ^{1}H or to $BF_3\cdot OEt_2$ as an external standard for ^{11}B and $^{11}B\{^1H\}$ NMR. Chemical shifts were reported in ppm and coupling constants in Hertz. Multiplet nomenclature is as follows: s, singlet; d, doublet; t, triplet; br, broad; and m, multiplet.

Synthesis of Me_2L2, H_2L2 and 2

1,7-Di(3-methylphenyl)-1,7-dicarba-*closo*-dodecaborane (Me2L2). The synthesis of the 1,7-di(3,5-dicarboxyphenyl)-1,7-dicarba-*closo*-dodecaborane ligand (*m*CB-H_4L_2) was adapted from the literature.[63] The procedure was carried out under a nitrogen atmosphere in a round-bottomed flask equipped with a magnetic stir bar. 500 mg (3.47 mmol) of *m*-carborane (mCB) was added to an oven-dried Schlenk flask. The flask was evacuated and backfilled with N_2 three times, and then 1,2-dimethoxyethane (40 mL) was added to the flask. Once the mCB was totally dissolved, 4.77 mL (1.6 M in hexane) of *n*-BuLi was added dropwise into the mixture at 0 °C. The mixture was then stirred at room temperature for 20 min, and then 1.2 g of CuCl was added to it. The mixture was stirred for 30 min, and then 1.4 mL (14.89 mmol) of pyridine and 1.04 mL (7.63 mmol) of 3-iodotoluene were added. The solution was heated and fluxed at 85 °C for 48 h. The cooled mixture was diluted with 100 mL of diethyl ether and allowed to stand for 2 h. The precipitate was filtered off, and the solution was washed with HCl (3 M) solution and water. The diethyl ether was removed by rotatory evaporation, providing a sticky solid that was filtered through a silica gel column (hexane : dichloromethane = 15 : 1). The filtrate was concentrated using a rotary evaporator to obtain Me_2**L2** as a white solid (yield: 41.2%).

$^1H\{^{11}B\}$ NMR (400 MHz, $CDCl_3$): δ = 2.37 (s, 6H, CH_3), 2.64 (br, 10H, BH), 7.16 (d, 4H, C_6H_4), 7.30 (s, 4H, C_6H_4); $^{11}B\{^1H\}$ NMR (400 MHz, $CDCl_3$): δ = −6.60 (s, 2B), −11.02 (s, 5B), −13.73 (s, 2B), −15.68 (s, 1B). IR (ATR; selected bands; cm^{-1}): ν 3062 (CH); 2919 (CH); 2599 (BH).

1,7-Di(3-carboxyphenyl)-1,7-dicarba-*closo*-dodecaborane (H2L2). The procedure was adapted from the literature.[63] 3 g (30 mmol) of CrO_3 was added in small portions to a stirred mixture of 648 mg (2 mmol) of Me_2**L2**, 30 mL of glacial acetic acid, 7.5 mL of acetic anhydride, and 1.5 mL of concentrated H_2SO_4. The dark green mixture was stirred at 20 °C for 2 hours, then poured into 100 mL of distilled water. A precipitate was formed, which was then filtered off and washed with distilled water to remove the green chromium residues. The off-white solid was recrystallized by dissolving it in Na_2CO_3 solution, filtering the solution, and then acidifying it with HCl (12 M) aqueous solution. The white precipitate that was formed was filtered off to obtain pure H_2**L2** (yield: 77.8%).

$^{1}H\{^{11}B\}$ NMR (400 MHz, DMSO-d_6): δ = 2.50 (br, 10H, B–H), 7.53 (d, 2H, C_6H_4), 7.97 (d, 2H, C_6H_4), 7.82 (d, 2H, C_6H_4), 8.01 (s, 2H, C_6H_4), 13.29 (br s, 2H, COOH); $^{11}B\{^{1}H\}$ NMR (400 MHz, DMSO-d_6): δ = −10.62 (br, 10B); IR (ATR; selected bands; cm^{-1}): 2603 (BH); 1686 (C═O from carboxylate).

$[Cu_2(L2)_2(MeOH)(H_2O)]$·DMA (2). $Cu(NO_3)_2{\cdot}3H_2O$ (7.5 mg, 0.03 mmol) and H2L2 (7.7 mg, 0.0.02 mmol) were dissolved in 2 mL of DMA/methanol/H_2O (1 : 2 : 1) with the help of sonication. The above mixture was transferred to an 8-dram vial and further heated at 85 °C in an oven for 48 h. Bluish crystals of 2 were collected and washed with DMA (yield based on the ligand: 38.4%). IR (ATR; selected bands; cm^{-1}): 2603 (BH); 1654 (C═O from DMA); 1615 (C═O from carboxylate). Elemental analysis, calculated: C 43.23, H 4.90, N 1.36; found: C 41.71, H, 4.78, N 1.42.

X-ray crystallography

Measured crystals were prepared under inert conditions immersed in perfluoropolyether as a protecting oil for manipulation. Suitable crystals were mounted on MiTeGen Mi-cromounts™, and these samples were used for data collection. Data for **2** were collected with a Bruker D8 Venture diffractometer with graphite monochromated CuKα (λ = 1.54178 Å, at 298(2) K). The data were processed with an APEX3 suite.[64] The structures were solved by Intrinsic Phasing using the ShelXT program,[65] which revealed the position of all non-hydrogen atoms. These atoms were refined on F^2 by a full-matrix least-squares procedure using anisotropic displacement parameters.[66] All hydrogen atoms were located in difference Fourier maps and included as fixed contributions riding on attached atoms with isotropic thermal displacement parameters that are 1.2- or 1.5-times those of the respective atoms. The Olex2 software was used as a graphical interface.[67] The contribution of a DMA disordered solvent molecule to the diffraction pattern could not be rigorously included in the model and was consequently removed with the mask tool implemented in Olex2 Molecular graphics that were generated using Mercury.[68] The crystallographic data for the reported structure were deposited with the Cambridge Crystallographic Data Center as supplementary publication no. CCDC 2119738.‡ A summary of the crystal data is presented in Table S1.‡

Catalytic performance of the aza-Michael mono-addition reaction

Acrylonitrile (0.144 mL, 2.2 mmol) and Cu-MOFs (10.3 mg, 0.02 mmol) were dispersed in 4 mL of methanol. Hexylamine (0.263 mL, 2.0 mmol) was then added into the above suspension and further stirred at room temperature for 60 min. Reaction conversion was monitored by withdrawing aliquots from the reaction mixture at different time intervals, quenching with diethyl ether, and drying over anhydrous $MgSO_4$ and analyzed by NMR. The product identity was confirmed by NMR.[48] The catalyst concentration was calculated with respect to the Cu/hexylamine molar ratio. The catalyst was recycled by centrifugation at 6000 rpm for 30 min. After washing with methanol and drying at 80 °C, the catalyst loss was monitored by the weight difference before and after each catalytic cycle.

3-(Hexylamino)propanenitrile (400 MHz, $CDCl_3$):[48] δ = 0.79 (m, 3H, CH_3), 1.20 (m, 6H, CH_2), 1.40 (m, 2H, CH_2), 2.47 (m, 2H, CH_2), 2.54 (br m, 2H, CH_2), and 2.85 (br m, 2H, CH_2).

Results and discussion

Synthesis and characterization

The reaction of $Cu(NO_3)_2$ and **L2** (Chart 1) in a 1 : 2 : 1 mixture of dimethylacetamide (DMA), methanol (MeOH) and water (H_2O) at 85 °C for 48 h afforded blue crystals of $[Cu_2(L2)_2(MeOH)(H_2O)]$·DMA (**2**). The IR spectrum showed characteristic broad B–H stretching bands of carborane (2603 cm^{-1}) and the C═O vibration of the carboxylate groups (Fig. S1‡). Single-crystal X-ray diffraction (Fig. 1 and Tables S1 and S2‡) patterns revealed the 1D network of **2**. Phase purity was confirmed by elemental analysis, powder X-ray diffraction (PXRD, Fig. S2‡) and thermogravimetric analysis (TGA; Fig. S3‡). The TGA curve of this material revealed good thermal stability as the framework is stable up to 300 °C. Activated **2** was proved to be non-porous under N_2 at 77 K and 1 bar. However, it was slightly porous to CO_2 (13.3 $cm^3\ g^{-1}$ at 0.9 bar; Dubinin–Raduskhevich surface area = 131 $m^2\ g^{-1}$; Fig. S4‡).

The basic unit of **2** is a Cu_2-paddle wheel motif of $[Cu_2(COO)_4]$ units (Fig. 1A). Each paddle wheel unit contains

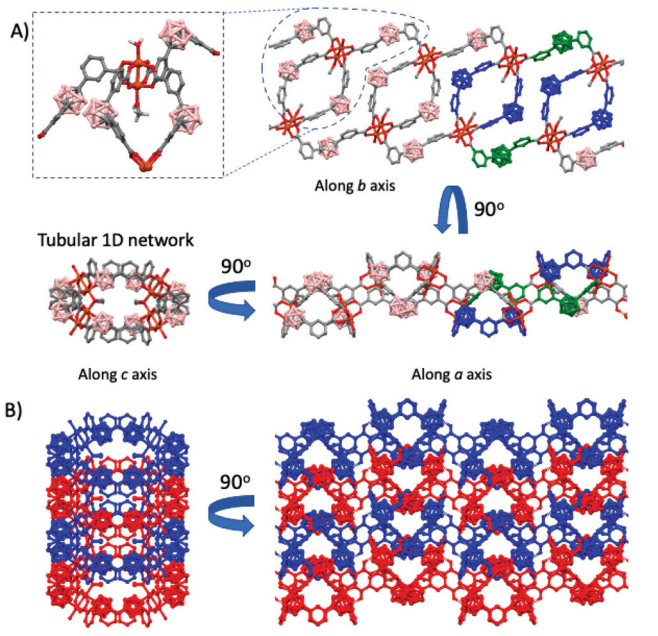

Fig. 1 X-ray structure of **2**. (A) View of the Cu_2-paddle wheel units with **L2** coordination and various perpendicular views of the 1D chain; blue and green colored **L2** represents two different conformations observed for the linker along the structure. (B) Two perpendicular views of the stacked 1D chains to provide the 2D structure; stacked 1D chains are colored red or blue for clarity. H atoms are omitted for clarity. Color code: B, pink; C, grey; O, red; N, blue; and Cu, orange.

four $L2^{2-}$ ligands, one water molecule and one methanol molecule, the latter two being located at the apical positions. The electron density corresponding to one free molecule of DMA was removed using the mask tool implemented in Olex2.[67] Cu–Cu distances in the paddle wheel units were 2.621 Å. Cu–OOC bond lengths ranged from 1.952 to 1.985 Å and Cu–O_{solv} bond lengths were 2.154 (MeOH) to 2.159 (H_2O) Å. The carborane **L2** linker showed two different conformations with a V-shape (OOC–CB centroid–COO ≈ 119 and 124°) and two non-coplanar phenyl rings for each conformation (55 and 74°, respectively; Fig. S5‡). Two of the more bent conformers of the **L2** linker bridge two Cu_2-paddle wheel units to create dimers (Fig. 1A). These dimers are then crosslinked by two of the wider conformers of **L2**, thus creating a kind of tubular 1D chain (Fig. 1A). The topological analysis reveals a uninodal net (Fig. S6‡) with a rare SP 1-periodic net (4,4)(0,2) topology defined by the point symbol of $(4^2{\cdot}6)$.[69,70] The observed 1D chain grows along the *c* axis. As can be seen in Fig. 1A, the coordinated methanol molecules are located toward the inside of the tubular chains while the coordinated water molecules are pointing toward the external surface of the tubular chains. No interpenetration of 1D chains is observed. Instead, the chains are stacked to provide 2D structures (Fig. 1B). Interchain hydrogen bonding was observed between the coordinated methanol proton and one of the carboxylate oxygen atoms of the adjacent chains (Cu(Me)O–H···O; H···O, 2.606 Å; OHO, 152.9°). The self-assembly of the 2D structures by intermolecular weak interactions provides 3D structures, as shown in Fig. S7.‡

Water stability

The related Cu structure with the more symmetrical **L1** ligand (Chart 1) provided a quite different topology. **1-Solv** exhibits a 4^4-grid topology by bending alternately above and below the plane containing paddle wheel [$Cu_2(COO)_4$] units to produce more corrugated 2D layers (Fig. S8‡).[62] The stacking of the 2D layers gives rise to the 3D structures of the compounds. Easy sliding of the 2D layers favors phase transitions on solvent exchange (from DFM to MeOH or CH_2Cl_2). We noted that water suspensions of **1** became blue colored quite rapidly, evidencing its instability in this solvent. Consequently, the PXRD patterns and optical microscopy images of **1** indicate a clear phase transition after being immersed in water for one week and complete amorphization and partial dissolution after two weeks (Fig. 2a and S9‡). **2** shows, however, quite remarkable stability in a variety of solvents, including methanol and water (Fig. 2b and Fig. S9–S12‡). **2** is stable in water for at least two months as confirmed by both PXRD and optical microscopy (Fig. 2b and Fig. S11 and S12‡). Remarkably, the crystals of **2** diffracted well after one month in water. Quite interestingly, the structure of **2** remained unaltered after being in water for such a long period, including the solvents (water and methanol) at the Cu_2-paddle wheel apical positions. **2** also shows stability in acidic and basic aqueous solutions (from 6 to 8; pH adjusted with HCl or KOH) for 24 h at room temperature (Fig. S13 and S14‡).

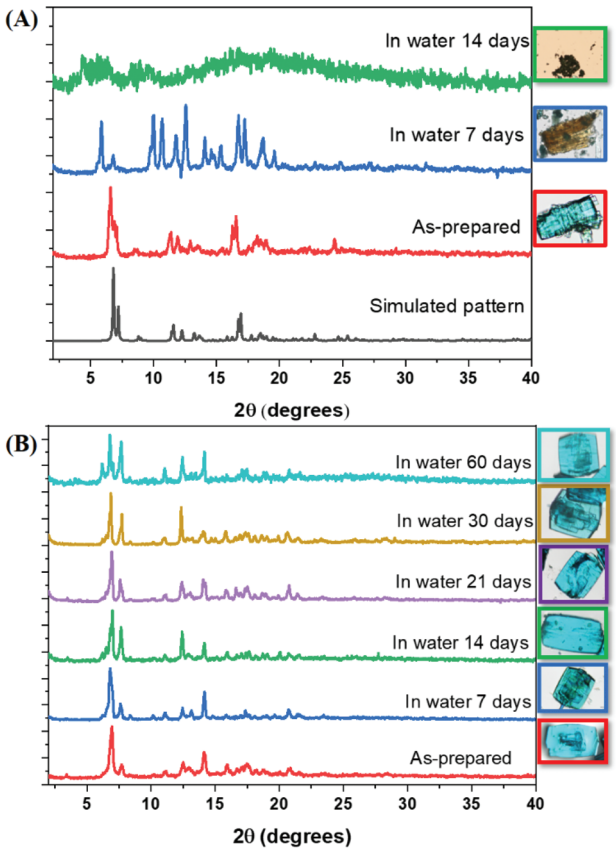

Fig. 2 A comparison of the PXRD patterns of **1** (A) and **2** (B) after being immersed in water for various time periods.

Aza-Michael addition reaction

MOFs are promising candidates as catalysts for various reactions.[15,71,72] However, in order to function effectively in reactions where water is involved, sufficient hydrothermal stability of the catalyst is vitally important. Hence, catalysts based on water stable MOFs stand out as they are capable of remaining robust and effective throughout the catalytic process. Having determined the different stabilities of **1** and **2** in water, we evaluated the performance of these two materials as heterogeneous catalysts for the model Aza-Michael addition reaction. The latter is one of the simplest and most effective approaches for synthesizing α,β-unsaturated carbonyl/nitrile compounds.[73–78] Due to the poor nucleophilicity of amines, the introduction of aqueous media with promoting agents is necessary for the aza-Michael addition reaction in some cases. Thus, we evaluated the activity of Cu centers in **1** and **2** as Lewis-acids in the aza-Michael mono-addition reaction of hexylamine and acrylonitrile to form 3-(hexylamino)propanenitrile as the model reaction (Fig. 3 and Experimental section).[78]

Both **1** and **2** provided complete conversion (>99%) after 1 hour at room temperature with 1 mol% catalyst loading, whereas the absence of any catalyst provides negligible conversion (Table S3‡). The catalytic activity is significantly improved over other 3D-Cu MOF catalysts that require 5 mol% loading

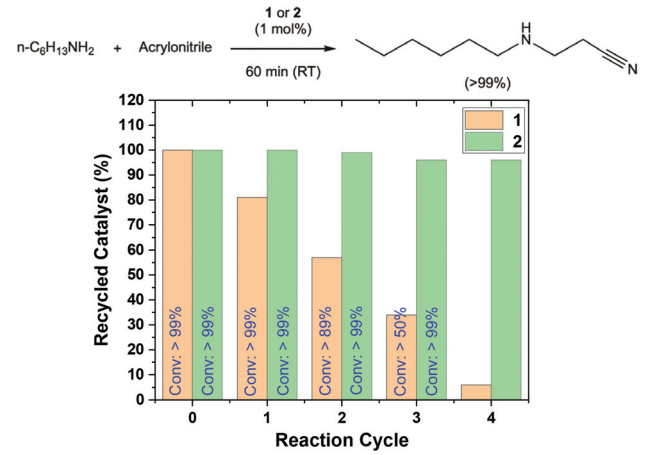

Fig. 3 Top: aza-Michael mono-addition reaction model in this work. Bottom: weight loss of catalysts (orange and green bars) and conversions (in blue) after various catalytic cycles.

for such high activity.[73,75] The heterogeneity of the catalysts and recyclability were tested for several cycles (Fig. 3). The solid materials were separated after each reaction by simple decantation, washed with methanol and dried at 80 °C. The recovered materials were reused several times to test their recyclability. As shown in Fig. 3, **1** loses both catalytic activity and weight after each cycle. In contrast, **2** can be reused four times without losing any significant activity or weight. These data reflect the heterogeneous nature of the catalyst and demonstrate the long-term chemical robustness and good catalytic performance of the new water-stable 1D Cu-MOF **2** in contrast to the less water-stable 2D Cu-MOF **1**. Such excellent catalytic performance has most probably originated from the high number of accessible Lewis-acid centers due to the 1D nature of **2** and the exceptional hydrolytic stability of this material.

Conclusions

We report the synthesis of a newly flexible *m*-carborane dicarboxylic linker 1,7-di(3-carboxyphenyl)-1,7-dicarba-*closo*-dodecaborane (**L2**) and the corresponding 1D Cu_2-paddle wheel coordination polymer **2**. The 1D structure of **2** contrasts with that of the related previously reported 2D Cu_2-paddle wheel coordination polymer **1**, formed with the more symmetric 1,7-di(4-carboxyphenyl)-1,7-dicarba-*closo*-dodecaborane (**L1**). **1** is stable in water for only one week, whereas **2** is stable in this solvent for at least two months. Regardless of its 1D structure, **2** shows remarkable stability in a variety of solvents and under pH conditions. Such hydrolytic stability is attributed to the combination of the arrangement of carborane moieties in the observed tubular 1D chains and their highly hydrophobic nature. Both **1** and **2** were used as efficient heterogeneous catalysts for the aza-Michael reaction of hexylamine with acrylonitrile to form 3-(hexylamino)propanenitrile as a model reaction. >99% conversions were achieved under mild conditions in the presence of only 1 mol% catalyst. In contrast to **1**, **2** can be separated from the reaction mixture by simple decantation and can be reused several times without significant degradation in catalytic activity or loss of the catalyst. The catalytic results show a clear improvement due to the higher hydrolytic stability of **2** against **1**.

The present work demonstrates how the selection of appropriate carborane-based linkers can better protect the Cu centers from water and therefore significantly increase the hydrolytic stability of the final coordination polymers. Our results also demonstrate the feasibility of using **2** as a recyclable solid Lewis acid catalyst for aza-Michael reactions and open new avenues for the application of 1D coordination polymers in catalysis.

Author contributions

Z. L.: syntheses and compound characterization, catalysis and figures; D. C.-L.: X-ray crystallography; J. F.: gas sorption characterization; C. V.: writing–review and editing; F. T.: writing–review and editing; and J. G. P: writing–original draft, validation of results and supervision.

Conflicts of interest

There are no conflicts to declare.

Acknowledgements

This work was financially supported by MICINN (PID2019-106832RB-I00), MICINN through the Severo Ochoa Program for Centers of Excellence for the FUNFUTURE (CEX2019-000917-S project) and the Generalitat de Catalunya (2017/SGR/1720). D. Ch.-L. acknowledges funding by project no. PGC2018-102047-B-I00 (MCIU/AEI/FEDER, UE). Zhen Li is enrolled in the UAB PhD program and acknowledges the China Scholarship Council (CSC) for his PhD grant (201808310071).

Notes and references

1 J. R. Long and O. M. Yaghi, *Chem. Soc. Rev.*, 2009, **38**, 1213–1214.
2 S. Kitagawa, R. Kitaura and S. Noro, *Angew. Chem., Int. Ed.*, 2004, **43**, 2334–2375.
3 S. L. James, *Chem. Soc. Rev.*, 2003, **32**, 276–288.
4 H. Li, M. Eddaoudi, M. O'Keeffe and O. M. Yaghi, *Nature*, 1999, **402**, 276–279.
5 R. Núñez, I. Romero, F. Teixidor and C. Viñas, *Chem. Soc. Rev.*, 2016, **45**, 5147–5173.
6 S. Dhaka, R. Kumar, A. Deep, M. B. Kurade, S.-W. Ji and B.-H. Jeon, *Coord. Chem. Rev.*, 2019, **380**, 330–352.

7 M. Du, Q. Li, Y. Zhao, C.-S. Liu and H. Pang, *Coord. Chem. Rev.*, 2020, **416**, 213341.
8 S. Rojas and P. Horcajada, *Chem. Rev.*, 2020, **120**, 8378–8415.
9 A. U. Czaja, N. Trukhan and U. Müller, *Chem. Soc. Rev.*, 2009, **38**, 1284–1293.
10 Y. Cui, Y. Yue, G. Qian and B. Chen, *Chem. Rev.*, 2012, **112**, 1126–1162.
11 H. Furukawa, K. E. Cordova, M. O'Keeffe and O. M. Yaghi, *Science*, 2013, **341**, 1230444.
12 H. Wang, Q.-L. Zhu, R. Zou and Q. Xu, *Chem*, 2017, **2**, 52–80.
13 W. P. Lustig, S. Mukherjee, N. D. Rudd, A. V. Desai, J. Li and S. K. Ghosh, *Chem. Soc. Rev.*, 2017, **46**, 3242–3285.
14 G. Minguez Espallargas and E. Coronado, *Chem. Soc. Rev.*, 2018, **47**, 533–557.
15 G. Chakraborty, I.-H. Park, R. Medishetty and J. J. Vittal, *Chem. Rev.*, 2021, **121**, 3751–3891.
16 N. C. Burtch, H. Jasuja and K. S. Walton, *Chem. Rev.*, 2014, **114**, 10575–10612.
17 N. U. Qadir, S. A. M. Said and H. M. Bahaidarah, *Microporous Mesoporous Mater.*, 2015, **201**, 61–90.
18 B. S. Gelfand and G. K. H. Shimizu, *Dalton Trans.*, 2016, **45**, 3668–3678.
19 E. Moumen, A. H. Assen, K. Adil and Y. Belmabkhout, *Coord. Chem. Rev.*, 2021, **443**, 214020.
20 X. Zhang, B. Wang, A. Alsalme, S. Xiang, Z. Zhang and B. Chen, *Coord. Chem. Rev.*, 2020, **423**, 213507.
21 T. He, X.-J. Kong and J.-R. Li, *Acc. Chem. Res.*, 2021, **54**(15), 3083–3094.
22 M. Ding, X. Cai and H.-L. Jiang, *Chem. Sci.*, 2019, **10**, 10209–10230.
23 J. Duan, W. Jin and S. Kitagawa, *Coord. Chem. Rev.*, 2017, **332**, 48–74.
24 C. Wang, X. Liu, N. Keser Demir, J. P. Chen and K. Li, *Chem. Soc. Rev.*, 2016, **45**, 5107–5134.
25 K. Jayaramulu, F. Geyer, A. Schneemann, S. Kment, M. Otyepka, R. Zboril, D. Vollmer and R. A. Fischer, *Adv. Mater.*, 2019, **31**, e1900820.
26 L.-H. Xie, M.-M. Xu, X.-M. Liu, M.-J. Zhao and J.-R. Li, *Adv. Sci.*, 2020, **7**, 1901758.
27 L. Gan, A. Chidambaram, P. G. Fonquernie, M. E. Light, D. Choquesillo-Lazarte, H. Huang, E. Solano, J. Fraile, C. Viñas, F. Teixidor, J. A. R. Navarro, K. C. Stylianou and J. G. Planas, *J. Am. Chem. Soc.*, 2020, **142**, 8299–8311.
28 J. Plesek, *Chem. Rev.*, 1992, **92**, 269–278.
29 M. Scholz and E. Hey-Hawkins, *Chem. Rev.*, 2011, **111**, 7035–7062.
30 R. N. Grimes, *Carboranes*, Academic Press, 2016.
31 S. Fujii, *MedChemComm*, 2016, **7**, 1082–1092.
32 A. Ferrer-Ugalde, E. J. Juárez-Pérez, F. Teixidor, C. Viñas and R. Núñez, *Chem. – Eur. J.*, 2013, **19**, 17021–17030.
33 F. Teixidor, G. Barberà, A. Vaca, R. Kivekäs, R. Sillanpää, J. Oliva and C. Viñas, *J. Am. Chem. Soc.*, 2005, **127**, 10158–10159.
34 A. M. Spokoyny, C. W. Machan, D. J. Clingerman, M. S. Rosen, M. J. Wiester, R. D. Kennedy, C. L. Stern, A. A. Sarjeant and C. A. Mirkin, *Nat. Chem.*, 2011, **3**, 590–596.
35 J. Poater, M. Solà, C. Viñas and F. Teixidor, *Angew. Chem., Int. Ed.*, 2014, **53**, 12191–12195.
36 J. Poater, C. Viñas, I. Bennour, S. Escayola, M. Solà and F. Teixidor, *J. Am. Chem. Soc.*, 2020, **142**, 9396–9407.
37 X. Zhao, Z. Yang, H. Chen, Z. Wang, X. Zhou and H. Zhang, *Coord. Chem. Rev.*, 2021, **444**, 214042.
38 Q. Xia, J. Zhang, X. Chen, C. Cheng, D. Chu, X. Tang, H. Li and Y. Cui, *Coord. Chem. Rev.*, 2021, **435**, 213783.
39 Y. Zhang, L. Wang, J. Hu, S. Duttwyler, X. Cui and H. Xing, *CrystEngComm*, 2020, **22**, 2649–2655.
40 Y. Zhang, J. Hu, R. Krishna, L. Wang, L. Yang, X. Cui, S. Duttwyler and H. Xing, *Angew. Chem.*, 2020, **59**, 17664–17669.
41 Y. Zhang, L. Yang, L. Wang, S. Duttwyler and H. Xing, *Angew. Chem., Int. Ed.*, 2019, **58**, 8145–8150.
42 L. Wang, W. Sun, Y. Zhang, N. Xu, R. Krishna, J. Hu, Y. Jiang, Y. He and H. Xing, *Angew. Chem., Int. Ed.*, 2021, **60**, 22865–22870.
43 J. Planas, F. Teixidor and C. Viñas, *Crystals*, 2016, **6**, 50.
44 F. Di Salvo, C. Paterakis, M. Y. Tsang, Y. Garcia, C. Viñas, F. Teixidor, J. G. Planas, M. E. Light, M. B. Hursthouse and D. Choquesillo-Lazarte, *Cryst. Growth Des.*, 2013, **13**, 1473–1484.
45 F. Di Salvo, M. Y. Tsang, F. Teixidor, C. Viñas, J. G. Planas, J. Crassous, N. Vanthuyne, N. Aliaga-Alcalde, E. Ruiz, G. Coquerel, S. Clevers, V. Dupray, D. Choquesillo-Lazarte, M. E. Light and M. B. Hursthouse, *Chem. – Eur. J.*, 2014, **20**, 1081–1090.
46 M. Y. Tsang, C. Viñas, F. Teixidor, J. G. Planas, N. Conde, R. SanMartin, M. T. Herrero, E. Dominguez, A. Lledos, P. Vidossich and D. Choquesillo-Lazarte, *Inorg. Chem.*, 2014, **53**, 9284–9295.
47 M. Y. Tsang, F. Teixidor, C. Viñas, D. Choquesillo-Lazarte, N. Aliaga-Alcalde and J. G. Planas, *Inorg. Chim. Acta*, 2016, **448**, 97–103.
48 J. Soldevila-Sanmartín, E. Ruiz, D. Choquesillo-Lazarte, M. E. Light, C. Viñas, F. Teixidor, R. Núñez, J. Pons and J. G. Planas, *J. Mater. Chem. C*, 2021, **9**, 7643–7657.
49 O. K. Farha, A. M. Spokoyny, K. L. Mulfort, M. F. Hawthorne, C. A. Mirkin and J. T. Hupp, *J. Am. Chem. Soc.*, 2007, **129**, 12680–12681.
50 Y.-S. Bae, O. K. Farha, A. M. Spokoyny, C. A. Mirkin, J. T. Hupp and R. Q. Snurr, *Chem. Commun.*, 2008, 4135.
51 O. K. Farha, A. M. Spokoyny, K. L. Mulfort, S. Galli, J. T. Hupp and C. A. Mirkin, *Small*, 2009, **5**, 1727–1731.
52 Y.-S. Bae, A. M. Spokoyny, O. K. Farha, R. Q. Snurr, J. T. Hupp and C. A. Mirkin, *Chem. Commun.*, 2010, **46**, 3478–3480.
53 A. M. Spokoyny, O. K. Farha, K. L. Mulfort, J. T. Hupp and C. A. Mirkin, *Inorg. Chim. Acta*, 2010, **364**, 266–271.
54 S.-L. Huang, Y.-J. Lin, W.-B. Yu and G.-X. Jin, *ChemPlusChem*, 2012, **77**, 141–147.
55 R. D. Kennedy, V. Krungleviciute, D. J. Clingerman, J. E. Mondloch, Y. Peng, C. E. Wilmer, A. A. Sarjeant,

R. Q. Snurr, J. T. Hupp, T. Yildirim, O. K. Farha and C. A. Mirkin, *Chem. Mater.*, 2013, **25**, 3539–3543.
56 D. J. Clingerman, W. Morris, J. E. Mondloch, R. D. Kennedy, A. A. Sarjeant, C. Stern, J. T. Hupp, O. K. Farha and C. A. Mirkin, *Chem. Commun.*, 2015, **51**, 6521–6523.
57 S. Rodríguez-Hermida, M. Y. Tsang, C. Vignatti, K. C. Stylianou, V. Guillerm, J. Pérez-Carvajal, F. Teixidor, C. Viñas, D. Choquesillo-Lazarte, C. Verdugo-Escamilla, I. Peral, J. Juanhuix, A. Verdaguer, I. Imaz, D. Maspoch and J. G. Planas, *Angew. Chem., Int. Ed.*, 2016, **55**, 16049–16053.
58 M. Y. Tsang, S. Rodríguez-Hermida, K. C. Stylianou, F. Tan, D. Negi, F. Teixidor, C. Viñas, D. Choquesillo-Lazarte, C. Verdugo-Escamilla, M. Guerrero, J. Sort, J. Juanhuix, D. Maspoch and J. G. Planas, *Cryst. Growth Des.*, 2017, **17**, 846–857.
59 F. Tan, A. López-Periago, M. E. Light, J. Cirera, E. Ruiz, A. Borrás, F. Teixidor, C. Viñas, C. Domingo and J. G. Planas, *Adv. Mater.*, 2018, **30**, 1800726.
60 Z. Li, J. Fraile, C. Viñas, F. Teixidor and J. G. Planas, *Chem. Commun.*, 2021, **57**, 2523–2526.
61 K. Tan, N. Nijem, P. Canepa, Q. Gong, J. Li, T. Thonhauser and Y. J. Chabal, *Chem. Mater.*, 2012, **24**, 3153–3167.
62 L. Gan, P. G. Fonquernie, M. E. Light, G. Norjmaa, G. Ujaque, D. Choquesillo-Lazarte, J. Fraile, F. Teixidor, C. Viñas and J. G. Planas, *Molecules*, 2019, **24**, 3204.
63 M. A. Fox, *Durham theses*, Durham Univ, 1991.
64 *Bruker APEX3. APEX3 V2019.1*, Bruker-AXS, Madison, WI, USA, 2019.
65 G. M. Sheldrick, *Acta Crystallogr., Sect. A: Found. Adv.*, 2015, **71**, 3–8.
66 G. Sheldrick, *Acta Crystallogr., Sect. C: Struct. Chem.*, 2015, **71**, 3–8.
67 O. V. Dolomanov, L. J. Bourhis, R. J. Gildea, J. A. K. Howard and H. Puschmann, *J. Appl. Crystallogr.*, 2009, **42**, 339–341.
68 C. F. Macrae, I. J. Bruno, J. A. Chisholm, P. R. Edgington, P. McCabe, E. Pidcock, L. Rodriguez-Monge, R. Taylor, J. van de Streek and P. A. Wood, *J. Appl. Crystallogr.*, 2008, **41**, 466–470.
69 S. A. Sotnik, R. A. Polunin, M. A. Kiskin, A. M. Kirillov, V. N. Dorofeeva, K. S. Gavrilenko, I. L. Eremenko, V. M. Novotortsev and S. V. Kolotilov, *Inorg. Chem.*, 2015, **54**, 5169–5181.
70 D.-H. Chen, L. Lin, T.-L. Sheng, Y.-H. Wen, S.-M. Hu, R.-B. Fu, C. Zhuo, H.-R. Li and X.-T. Wu, *CrystEngComm*, 2017, **19**, 2632–2643.
71 Ü. Kökçam-Demir, A. Goldman, L. Esrafili, M. Gharib, A. Morsali, O. Weingart and C. Janiak, *Chem. Soc. Rev.*, 2020, **49**, 2751–2798.
72 A. Bavykina, N. Kolobov, I. S. Khan, J. A. Bau, A. Ramirez and J. Gascon, *Chem. Rev.*, 2020, **120**, 8468–8535.
73 S. Bhattacharjee, A. A. Shaikh and W.-S. Ahn, *Catal. Lett.*, 2021, **151**, 2011–2018.
74 A. H. Chughtai, N. Ahmad, H. A. Younus, A. Laypkov and F. Verpoort, *Chem. Soc. Rev.*, 2015, **44**, 6804–6849.
75 L. T. L. Nguyen, T. T. Nguyen, K. D. Nguyen and N. T. S. Phan, *Appl. Catal., A*, 2012, **425–426**, 44–52.
76 X. Ai, X. Wang, J. Liu, Z. Ge, T. Cheng and R. Li, *Tetrahedron*, 2010, **66**, 5373–5377.
77 P. R. Krishna, A. Sreeshailam and R. Srinivas, *Tetrahedron*, 2009, **65**, 9657–9672.
78 G. Bosica and R. Abdilla, *Molecules*, 2016, **21**, 815.